

Laboratory Experiment on Failure of Embankment

Adrin Tohari*, Makoto Nishigaki ** and Mitsuru Komatsu*

(Received January 6 , 2000)

Failures of railway embankments in Japan usually occur during rainfall period due to the rise of water level in the embankments. Laboratory experiments were carried out to elucidate the initiation of failure of embankment under the rise of water level. The changes in pore-water pressure were monitored during the rise of water table and at the initiation of failures. The experiment results showed that main failure of embankment was initiated by development of localized unstable area at the toe of the embankment models during the rise of water level. This indicates that failure of embankments was a consequence of instability of the toe of the slope induced by saturation process under drained condition.

Key words: *embankment, failure process, seepage face, toe failure, overall instability*

1 INTRODUCTION

Embankments are very common earth structures constructed for railway foundation in Japan. During heavy rainfall season, many embankments frequently experience instability leading to the failure of the embankment that can distract the railway network and threaten the life of the onboard passengers and the surrounding residences.

Recently, some investigations have been carried out to study the condition leading to the failure of embankment under rainfall (Yamasaki et al, 1996; Ejigawa et al, 1998; Kato and Sakajo, 1999; Sakajo and Kato, 1999). Their study indicated that stability problem might occur on the embankment due to the rise of groundwater level, and the stability was influenced by seepage properties of the embankment soil.

Although the main factor causing failure of the embankments has been recognized, however, the actual process of failure initiation is still not clear. The understanding on failure initiation is essential for performing analysis and taking subsequent measures to prevent failures in the embankments.

The objective of the work presented in this Paper was to elucidate the process leading to failure initiation of embankment during water infiltration and the critical influence of seepage on failure initiation.

*Doctorate student, the Graduate School of Natural Science and Technology, Okayama University.

**Department of Environmental Design and Civil Engineering, Faculty of Environmental Science and Technology, Okayama University.

2 EXPERIMENTAL PROGRAM

Failure was induced in a number of 1-m high soil embankments by raising water level within the embankments. Prior to the first two experiments, a water level of 20 cm was introduced to produce initial water level across the base of each embankment from a constant head tank.

Three different modes of raising the water level in the embankment were considered in the experiments. In the first experiment, slow rise of water level was introduced to the embankment model from constant head tank at the rate of 5cm/hr. Second experiment considered a condition of rapid water level increase at the rate of 0.63cm/min. In the third experiment, rainfall at intensity 100mm/hr was simulated to raise water level in the embankment model.

Table 1 Properties of river sand

D ₁₀ (mm)	D ₆₀ /D ₁₀	Density of particle, ρ_s (gr/cm ³)	K _s (cm/s)	Cohesion (KPa)
0.175	7.14	2.69	0.029	0.0103

3 EXPERIMENTAL APPARATUSES

3.1 Soil Properties

In all experiments, river sand was used for the embankment model. Soil particles vary from fine sand

to coarse sand. The properties of river sand determined by laboratory experiments are summarized in **Table 1**.

3.2 Slope failure tank

The slope failure tank as the basic apparatus and the profile of the embankment model are shown in shown schematically in **Fig. 1**. This large metal tank was designed to accommodate 1-m high soil slope that could be brought to failure by seepage of water towards the toe. The dimensions of embankment model were chosen to reduce the effects of side friction limit (width and height ratio of 1.0), while keeping the volume to practical. The slope angle of 45° is close to the angle of repose of 50° . To generate an impervious boundary at the end of the slope model, a 1 cm acrylic board of 25 cm height was secured at the down slope end. The properties of the embankment models for each experiment are given in **Table 2**.

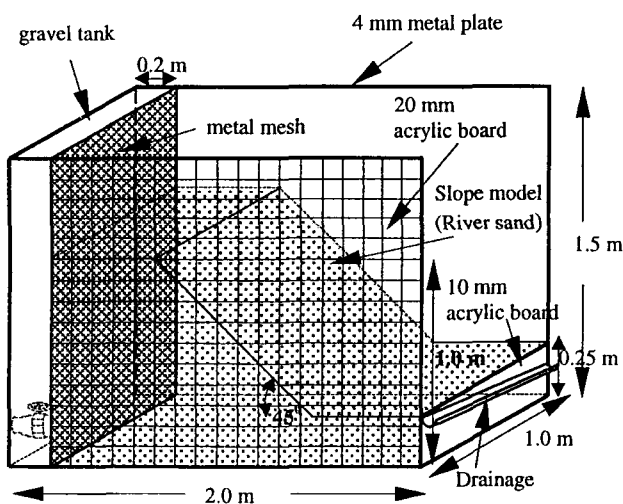


Fig. 1 Slope failure tank

The tank was facilitated with an acrylic observation window for pressure and deformation facilitated with embankment profile, grids, transducer holes and tracer injection holes at several points. During experiments, blue tracers were injected through the holes using ordinary syringes to visualize the flow lines within the embankment profile.

Table 2 Properties of experimental embankment models

Exp. No	Dry density, ρ_d (gr/cm ³)	Void ratio	Initial moisture content
1	5.0355	0.875	0.074
2	5.0265	0.909	0.066
3	5.1319	0.882	0.081

Water was allowed to enter the slope from the constant head tank through a coarse gravel-filled tank with porous sheet outlets to generate an initial lateral inflow. To inhibit direct sliding of the base along the soil/floor interface, a thin layer of sand was created over the floor after the glue being applied on the floor of the tank.

3.3 Pore-water pressure transducers

Eight pore-water pressure transducers were mounted in custom fitting through the observation window with porous cup submerged about 5mm within the soil itself to ensure effective measurements of rapid change in pore-water pressure. Each of the transducers was logged at approximately 1minute intervals. **Fig. 2** shows the configuration of pressure transducers.

3.4 Rainfall simulator

To induce the change in pore-water pressure and the failure due to rainfall infiltration in experiment 3, a rainfall simulator was set up above the embankment model. The simulator was designed to produce an effective rainfall intensity to bring about pore-water pressure changes and failure. It mainly consisted of the sprayer arms, sprayers and flow meter. The sprayers were made up of a transparent plastic pipe of 10 mm in diameter around which four holes of 1 mm in diameter were drilled in. Due to fluctuation of water pressure in the water supply, the amount of water flowing into the sprayer arms was carefully controlled through a valve to give a rainfall intensity of approximately 100 mm/hr. As the simulated rainfall would introduce surface erosion, the entire surface of slope model was covered by a plastic net to reduce this effect.

3.5 Sand placement

Prior to placement, the sand sample was mixed to give an approximately 5% water content using turbo mixer for each experiment. Average moisture content was determined from ratio of total amount of water to total dry sand used to construct the slope profile. Subsequently, the sand was placed in a series of horizontal layers of 5 cm thick to the full width of the tank before being tampered using a hand-made wood board tamper to give a slight compaction throughout the slope profile. Average dry density of the profile calculated from the total density and average moisture content was used to determine void ratio for each slope

profile (Table 2). Overall view of the tank and constructed slope profile is shown in Fig. 2.

3.4 Photography

A video camera was set up in front of the slope face to give a better view and complete record of saturation, failure initiation and movement. A 35-70 mm auto focus camera was used to record the flow lines, slope profile before and after failure, and displacement of sliding block.

dimensional nature of the overall failure processes are illustrated schematically in Fig. 4.

Table 3 Slope Toe Saturation

Exp. No.	Time for Toe Saturation (min)	Water Level at the back of embankment (cm)
1	73	29.7
2	10	51.95
3	54	24.0

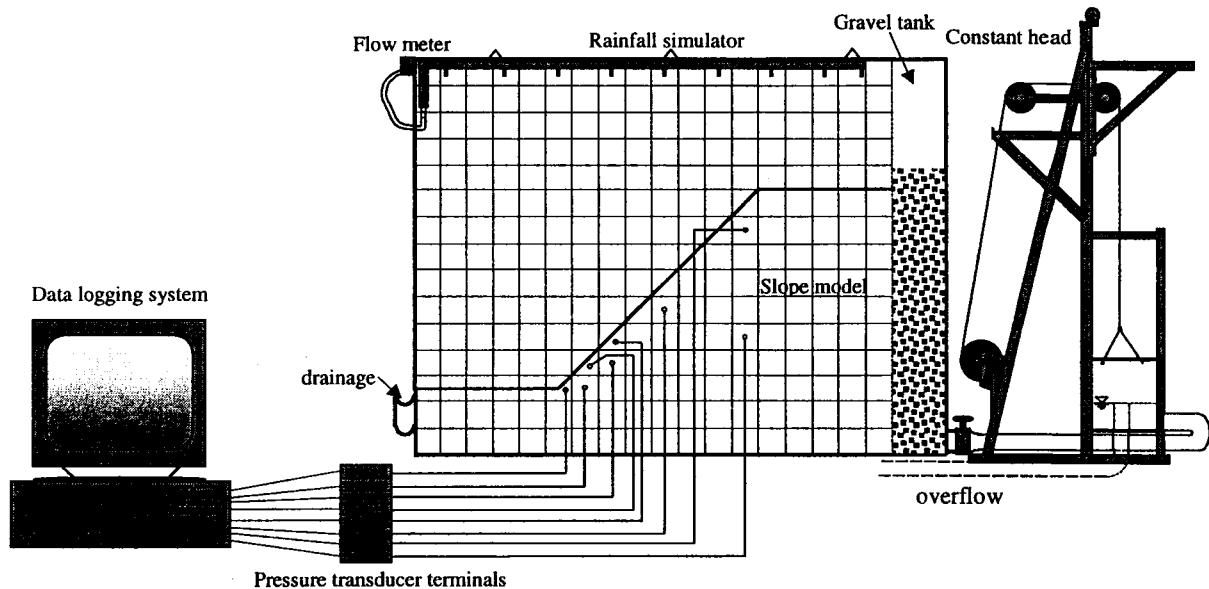


Fig. 2 Overview of set up of instrumentation

4 FAILURE DEVELOPMENT

4.1 Overall failure process

Embankment model under slow rise of water level failed by multiple regressive non-circular slips. The whole process required 20 to 60 minutes for slope wetting and a few minutes for collapse. In contrast, embankment models under quick rising and rainfall infiltration failed by shallow non-circular slide over a period of 16 minutes and 90 minutes from the start of the experiment, respectively. Failure process for each case is covered in detail in this section. The detail history of failure varied with each experiment and needs to be interpreted in association with the pore-water pressure records and the mode of rising water level.

The duration for toe saturation in each experiment is tabulated in Table 3. It is worth-noting that wetting front advanced more rapidly under quick raising condition compared with the other two conditions. The three

Failures of each embankment model commenced by toe saturation and development of tension crack at the toe of the embankment. In experiments 2 and 3, tension cracks were also developed at the top of the embankment before toe saturation. In experiment 1, retrogressive sliding was preceded by localized shallow failures at the toe following the development of seepage face. The next sliding did not initiate the previous slab had virtually come to rest and until the next rise of water level.

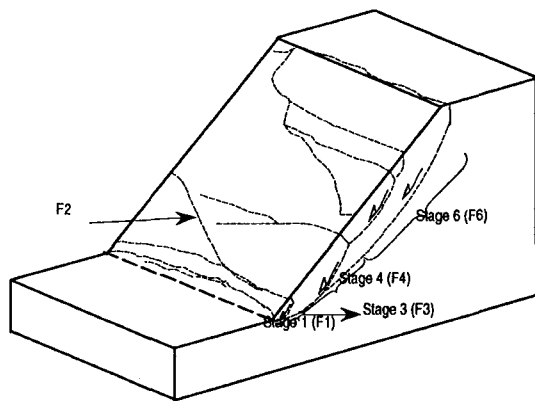
For comparison, development of at tension crack at the toe and the top of the slope generated instability to the whole portion of the slope in experiments 2 and 3. Main failure took place a few seconds after toe failure.

4.2 Failure modes

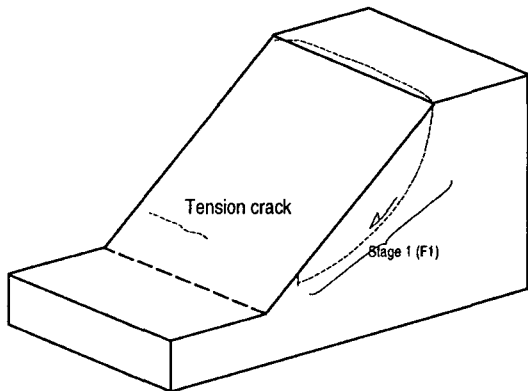
Failure modes observed in all of experiments are summarized in Fig. 5. Most dominant mode of failure deduced from the experiments is shallow non-circular

slide, frequently retrogressive with failure surface cut through the slope toe.

Although placement conditions for all experiments were as nearly identical as possible, the failure modes were obviously different. It is believed that mode of raising water level in the slope controlled the failure modes. Experiment 1 failed by shallow retrogressive sliding rather than non-circular slide apparent in experiments 2 and 3. However, it is interesting to note that all failures were preceded by toe failure. This indicated that the occurrence of failures observed in all experiments was due to the loss of lateral support resulting from the earlier stage of failures.



Experiment 1



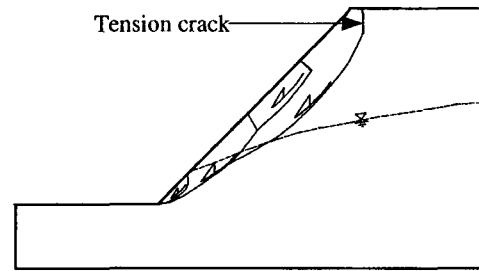
Experiment 2, 3

Fig. 4 Overall failure sequences

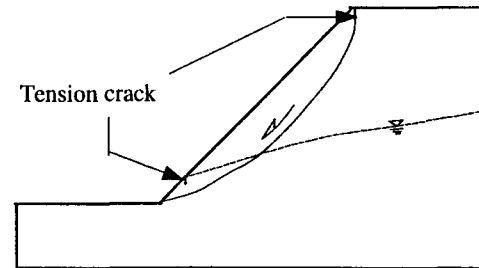
5 PORE-WATER PRESSURE

Pore-water pressure records during each experiment, as shown in Fig. 6 to 8, increased throughout the experiments in response to the advancing wetting fronts. Saturation is indicated by initially negative pore-water pressures increasing to zero. It should be noted that times representing initiation of the different stages of failure

was determined from the observations and the video and camera records.



Retrogressive non-circular sliding (experiment 1)



Shallow non-circular sliding (experiment 2, 3)

Fig. 5 Summary of failure modes for all experiments

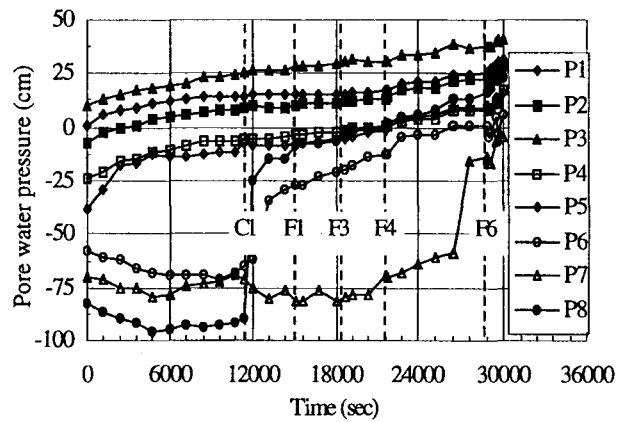


Fig. 6 Overall pore-water pressure changes, experiment 1

Pore-water pressure records during experiment one showed that pore-water pressures increased slowly. Near the slope surface transducer located near the toe, (P3) indicated the progress development of seepage face throughout the experiment that contributed to the occurrences of most failures (Fig. 6). For comparison, the advancing wetting front resulted initially in significantly rapid increase in pore-water pressures to positive value throughout experiments 2 and 3 (Fig. 7 and 8). Transducers located near the slope surface (P1-P3) showed pore-pressure increases to positive values prior to the occurrence of slope failure. This gave the

indication that failure initiation could be associated with the development of seepage face.

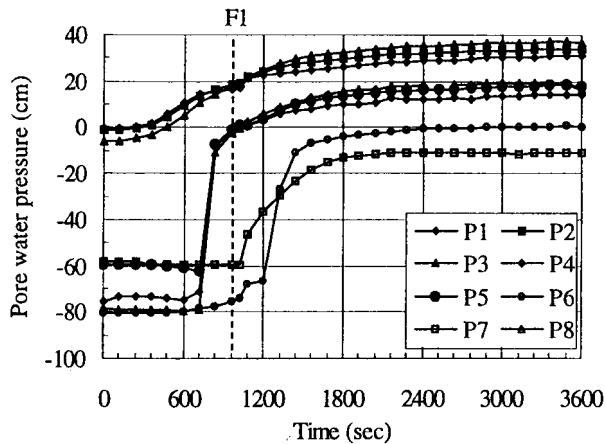


Fig. 7 Overall pore-water pressure changes, experiment 2

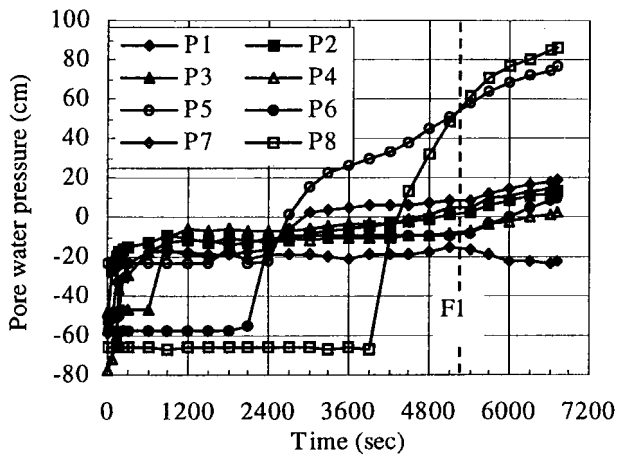


Fig. 8 Overall pore-water pressure changes, experiment 3

6. DISCUSSION

This discussion focuses first on some general inferences about the critical influence of seepage face on the initiation of failure of embankment. The principal result of our experiments showed that failure initiation process was associated with toe saturation and formation of seepage face and was independent upon the mode of raising the water level. The experiments also indicated that the shallow non-circular failure was the most dominant failure mode.

The detailed observations of failure process and development had indicated the initiation of failure on the embankment under water level rise was always preceded by seepage-induced failure of the toe area. Stated another way, water seepage was responsible for failure initiation. Under the effect of the groundwater seepage, the increase

of failure potential predominantly occurred in the near-surface region, and the increases were particularly significant near the embankment toe. This contradicts some theoretical hypotheses that failure starts with a slip circle mechanism. Therefore, the idea to analyze the stability of embankment under rise of groundwater level should have considered the influence of groundwater seepage within the embankment. The example of analytical approach to assess the effect of groundwater seepage on the potential for slope instability can be referred to Nishigaki et al (1996) among others.

The overall failure initiation and mechanism owing to the action of seepage forces upon the toe area clearly illustrates the critical influence of failure of the toe of a cohesionless embankment on overall instability, and the importance of effective toe drainage in preventing premature, retrogressive sliding due to locally high seepage pressures. The use of unsaturated seepage numerical analysis would assist one to determine the location where seepage face would develop.

7. CONCLUSIONS

The results of this experimental study support the following conclusions.

- (1) Under the seepage effect, the most dominant mode of failure of embankment was shallow non-circular sliding, often retrogressive.
- (2) Failure of embankment was initiated by the development of highly localized unstable toe area under drained condition.
- (3) The failure of toe region resulted in the loss of lateral support for the slope to be stable, and was subsequently proceeded by the occurrence of main failure.
- (4) The experiments suggested the prevention of premature seepage-induced failure by effective drainage on seepage area to maintain overall stability of the embankment.

REFERENCES

- Ejigawa, E., Nakamura H., Hasada S., Furuyama S. and Hirayama T. (1998): A case study of stability analysis of embankment using seepage flow analysis. *Proc. 34th Annual Japanese National Conference on Geotechnical Engineering*, vol. 2, pp. 2123-2124. (in Japanese).
- Kato, K. and Sakajo, S. (1999): Seepage analyses of embankments on Tokaido-Shinkansen in long term

rainfalls. *Proc. International Symposium on Slope Stability Engineering*, vol. 1, pp. 521-526.

Nishigaki, M., Tohari, A. and Komatsu, M.: Stress and seepage vector system on stability of hillslope. *Proc. China/ Japan International Conference on Water Environment and Disaster Prevention*, pp. 160-166.

Sakajo, S. and Kato, K. (1999): Failure analyses of embankments on Tokaido-Shinkansen in heavy rainfalls. *Proc. International Symposium on Slope Stability Engineering*, vol. 1, pp. 527-532.

Yamasaki, S., Sugiyama, T., Okada, K., Muraishi, H. and Akiyama, Y. (1996): Classification of rainfall patterns on slope collapses along railways. *Proc. 31st Annual Japanese National Conference on Geotechnical Engineering*, vol. 2, pp. 1993-1994. (in Japanese).